

Characterization of on-off intermittency

J. F. Heagy

Naval Research Laboratory, Washington, D.C. 20375-5000

N. Platt and S. M. Hammel

Naval Surface Warfare Center, 10901 New Hampshire Avenue, Silver Spring, Maryland 20903-5000

(Received 24 June 1993)

The recently reported behavior known as “on-off intermittency” [N. Platt, E. A. Spiegel, and C. Tresser, *Phys. Rev. Lett.* **70**, 279 (1993)] is investigated in a class of one-dimensional maps that are multiplicatively coupled to either random or chaotic signals. Specific attention is paid to the conditions for the onset of intermittent behavior, the distribution of laminar phases, and the mean laminar phase as a function of the coupling strength. An exact expression is obtained for the distribution of laminar phases in the case of uniformly distributed random driving. A universal asymptotic $-3/2$ power-law distribution is proven to hold for a large class of random driving cases. Power-law scaling of the mean laminar phase as a function of coupling strength near onset is predicted for random driving, with a critical exponent of -1 . Numerical studies with chaotically driven maps reveal similar behavior to random driving cases and suggest the need for a systematic study of “chaotic walks.”

PACS number(s): 05.45.+b, 03.20.+i

I. INTRODUCTION

Recently, a type of intermittent behavior known as “on-off intermittency” has been reported [1]. The behavior derives its name from the characteristic two-state nature of the intermittent signal. The “off” state is nearly constant, and can remain so for very long periods of time. These events are known as laminar phases, a term used to describe these events in other intermittency studies [2–4]. The “on” state is a burst, departing quickly from, and returning quickly to, the off state. Platt, Spiegel, and Tresser [1] have reported this behavior in a set of five coupled ordinary differential equations (which reduce to a set of equations equivalent to the Lorenz equations [5] in a particular limit) and in a driven piecewise linear map. The authors also present a geometric mechanism for the intermittent behavior, which clearly distinguishes on-off intermittency from other known types of intermittency: Pomeau and Manneville types I, II, and III [2–4,6] and crisis-induced intermittency [7,8].

In this paper we focus on the statistical properties of on-off intermittent signals, paying particular attention to the distribution of laminar phases and the mean laminar phase as a function of a system parameter. We develop the necessary theory for a simple class of driven maps that includes the map studied in [1]. Despite the simplicity of these systems, we believe they capture the essential dynamical features of on-off intermittency.

The outline of this paper is as follows: In Sec. II we introduce the class of maps to be studied. The conditions for the onset of intermittent behavior are derived. Numerical examples with both random driving and chaotic driving are presented to illustrate the onset predictions. Section III is devoted to the distribution of laminar phases for random driving. For uniform random driving, an exact analytic form for this distribution is derived. At

onset, the asymptotic form of this distribution is shown to be a power law with exponent $-\frac{3}{2}$. In Sec. IV we employ random-walk methods to prove the universality of power-law falloff at onset for a large class of random driving choices. In Sec. V numerical studies with chaotic driving are presented that show the same power-law behavior. In Sec. VI the mean laminar phase is studied as a function of the coupling strength. Near onset, both random and chaotic driving cases display power-law scaling of the mean laminar phase as a function of the coupling parameter, with a critical exponent of -1 . This is shown analytically for the uniform random driving case. Finally, in Sec. VII we summarize and discuss our results. The notion of a chaotic walk is introduced in an effort to understand the similarities between the random and chaotic driving cases. We also discuss the features of on-off intermittency in relation to other theories of intermittency.

II. A SIMPLE ON-OFF INTERMITTENT SYSTEM

The basic mechanism underlying the on-off intermittency investigated in Ref. [1] is the repeated variation of one dynamical variable through a bifurcation point of another dynamical variable. The first variable acts as a time-dependent parameter, while the response of the second variable comprises the intermittent signal. Here we incorporate this mechanism in a simple class of systems—parametrically driven one-dimensional maps. On-off intermittency can be achieved in these maps with both random and chaotic parameter variations.

The maps we study are of the form

$$y_{n+1} = z_n f(y_n), \quad (1)$$

where $f(0)=0$, $\partial f(y)/\partial y|_0 \neq 0$, and the variable z_n comes from a chaotic or a random process with density function

$\rho_z(z)$ [9]. We assume the function f is such that the solutions of Eq. (1) are bounded for all time.

As an example, take $f(y_n) = y_n(1 - y_n)$ and $z_n = ax_n$, where x_n is a random variable in the interval $[0,1]$ with uniform distribution and $a > 1$. In this case map (1) is a logistic map with random parameter. This map is a special case of a map studied by Linz and Lücke [10]. The map instantaneously passes through a transcritical bifurcation at $y = 0$ whenever $z_n = 1$ (see Fig. 1). Figure 2 shows two representative time series for this map; Fig. 2(a) is for $a = 2.6$, while Fig. 2(b) is for $a = 2.8$. Each time series is of length 10 000. The initial conditions and random number generator seeds [11] were the same for each case and in each case the transient had length zero. The time series of Fig. 2(a) eventually approaches zero and remains there, while that of Fig. 2(b) continues to oscillate as $n \rightarrow \infty$. The second time series displays the hallmark of on-off intermittent behavior—long periods of nearly constant signal interrupted by short-lived larger amplitude bursts. This time series is said to be *beyond the onset* of intermittent behavior.

In this paper we will focus primarily on the small-amplitude events in the vicinity of the fixed point $y = 0$, between the intermittent bursts; these events are known as *laminar phases*. Longer laminar phases usually contain exceptionally small values. The dynamics of a laminar phase is therefore almost completely determined by the linear part of the map. We emphasize that this type of intermittent behavior is distinct from Pomeau-Manneville type-I, -II, and -III intermittency [2–4,6], as well as crisis-induced intermittency [7,8]. These types of intermittency occur for *fixed* values of the bifurcation parameter, while the bifurcation parameter in on-off intermittency is a dynamical variable. On-off intermittent signals, as will be shown below, also have a distinct statistical nature. The intermittent behavior displayed above is somewhat akin to a phenomenon studied by Yu, Ott, and Chen [12,13]; however, the quantitative features are distinct. A more detailed comparison is given in Sec. VII.

Our first objective is to understand the conditions for the onset of intermittent behavior in map (1). The fixed point at $y = 0$ can destabilize only for $z [\partial f(y)/\partial y]_{y=0} > 1$. By absorbing $[\partial f(y)/\partial y]_{y=0}$ into the scale of z (e.g., through the parameter a), one can always choose $[\partial f(y)/\partial y]_{y=0} = 1$. Expanding $f(y)$ about $y = 0$ then gives

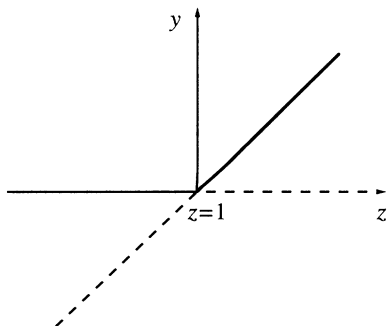


FIG. 1. Transcritical bifurcation of Eq. (1) as z passes through 1.

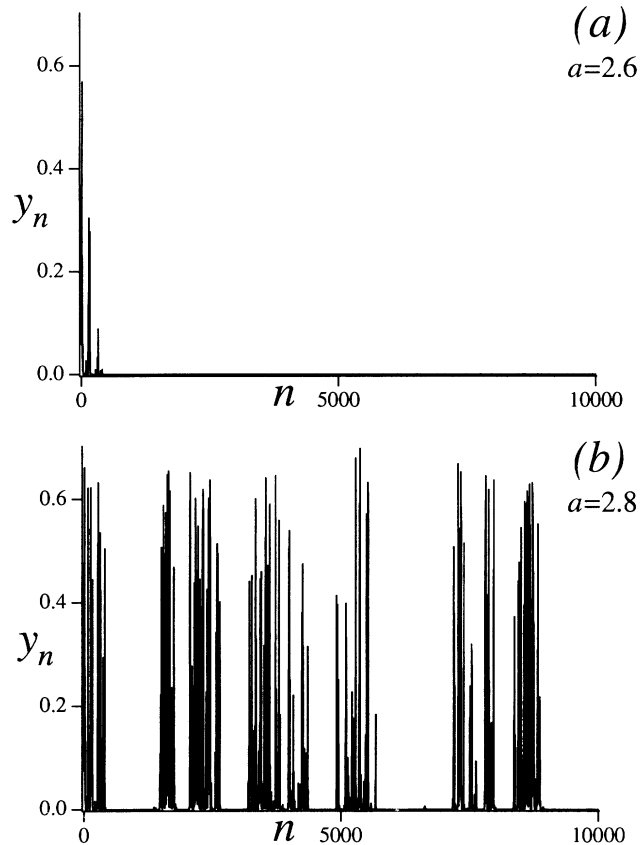


FIG. 2. Time series of driven logistic map with uniform random forcing: (a) below intermittency threshold at $a = 2.6$ and (b) above intermittency threshold at $a = 2.8$.

$$y_{n+1} = z_n(y_n + O(y_n^2)). \quad (2)$$

The intermittent phenomena observed above and throughout this paper are assumed to be controlled by the linear stability or instability of the fixed point at $y = 0$. Therefore, we keep only the leading order term in (2) in the stability analysis that follows. The nonlinear terms, as in the logistic map example, serve only to bound or *reinject* the dynamics back toward small values of y ; nonlinearity is therefore essential for *sustaining* the intermittent behavior, but not for initiating the intermittent bursts. In Sec. IV we give an alternate interpretation of the stability condition derived below that provides additional justification for the linear stability assumption. Further justification comes from the agreement between the theoretical onset predictions and the results of numerical experiments.

The solution of (2), keeping only the linear term in y_n , is

$$y_n = \prod_{j=0}^{n-1} z_j y_0. \quad (3)$$

The long-term behavior of y_n is determined by the asymptotic behavior of the random product

$$P_n = \prod_{j=0}^{n-1} z_j, \quad (4)$$

whose natural logarithm is given by

$$\ln P_n = \sum_{j=0}^{n-1} \ln z_j \sim n \langle \ln z \rangle . \tag{5}$$

The last relation in (5) follows from the law of large numbers [assuming that $\langle \ln z \rangle$ exists]. The average of $\ln z$ can be computed through the phase-space average

$$\langle \ln z \rangle = \int_{z_L}^{z_U} \rho_z(z) \ln z \, dz , \tag{6}$$

where z_L and z_U are the lower and upper limits of z [14]. The asymptotic solution of (3) is then given by

$$y_n \sim e^{n \langle \ln z \rangle} y_0 . \tag{7}$$

Here it is understood that y_n is small enough to be governed by the linearized map. From (7) it follows that the condition for the onset of intermittent behavior is $\langle \ln z \rangle = 0$ (this relation is also derived in [9]). For $\langle \ln z \rangle > 0$, $y = 0$ is, on average, exponentially unstable. This instability is the source of the intermittent bursts; however, due to the statistical nature of the driving signal, the instability does not preclude the occurrence of long orbit segments in the neighborhood of $y = 0$ (i.e., laminar phases). For the above example with $\rho_z(z) = 1$, Eq. (6) yields $\langle \ln z \rangle = \ln a - 1$, which gives $y_n \sim (a/e)^n y_0$. The critical value of a for the onset of intermittent behavior is therefore

$$a_c = e = 2.71828 \dots$$

This explains the qualitative difference between Figs. 2(a) and 2(b).

Experimental parameters are not always free to undergo large deviations. For this reason we also consider the onset criterion in the more general case when there is a constant offset in the variable z_n ; $z_n = b + ax_n$. This case permits smaller parameter variations a as the offset b approaches 1. The onset condition for this case leads to the expression

$$\begin{aligned} \langle \ln z \rangle &= \frac{1}{a} \int_b^{b+a} \ln z \, dz \\ &= \frac{1}{a} [(b+a) \ln(b+a) - a - b \ln b] = 0 . \end{aligned} \tag{8}$$

Figure 3 is a plot of the critical curve in the b - a plane for the onset of intermittency in this case.

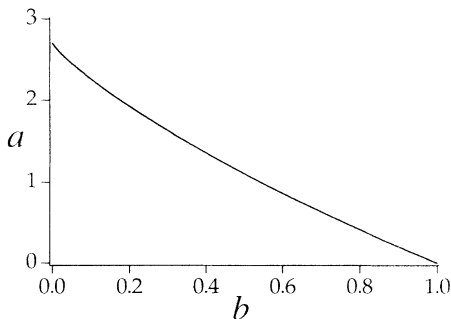


FIG. 3. Critical value of a for onset of intermittency as a function of the constant offset b .

Random driving is not necessary for on-off intermittency to occur; on-off intermittency also occurs in map (1) when the parameter z_n varies chaotically. The response of nonlinear systems to chaotic driving signals is currently a topic of much interest [15–18]. The study of these systems is expected to be useful in the analysis of coupled autonomous systems, since chaotic driving represents the limiting case where the inertia of one degree of freedom approaches infinity (the one-way coupling limit). A thorough understanding of this limiting case can yield insight into the more general two-way coupling problem.

We consider a simple example of map (1) with chaotic driving, again choosing $f(y_n) = y_n(1 - y_n)$ and $z_n = ax_n$, but now with $x_{n+1} = 2x_n \text{ mod } 1$ [19]. Except for a measure-zero set of initial conditions, the variable x_n has uniform distribution in $(0,1)$ [20]. The onset condition is therefore identical to the uniform random driving case discussed above, namely, $a_c = e$ [21]. Figures 4(a) and 4(b) show two time series of this map started from identical initial conditions for $a = 2.6$ and 2.8, respectively. The strong similarity of these time series to those of Figs. 2(a) and 2(b) should be noted. Similar results are found when the chaotic driving is provided by the tent map:

$$x_{n+1} = T(x_n) = \begin{cases} 2x_n, & 0 \leq x_n \leq \frac{1}{2} \\ 2 - 2x_n, & \frac{1}{2} \leq x_n \leq 1 . \end{cases} \tag{9}$$

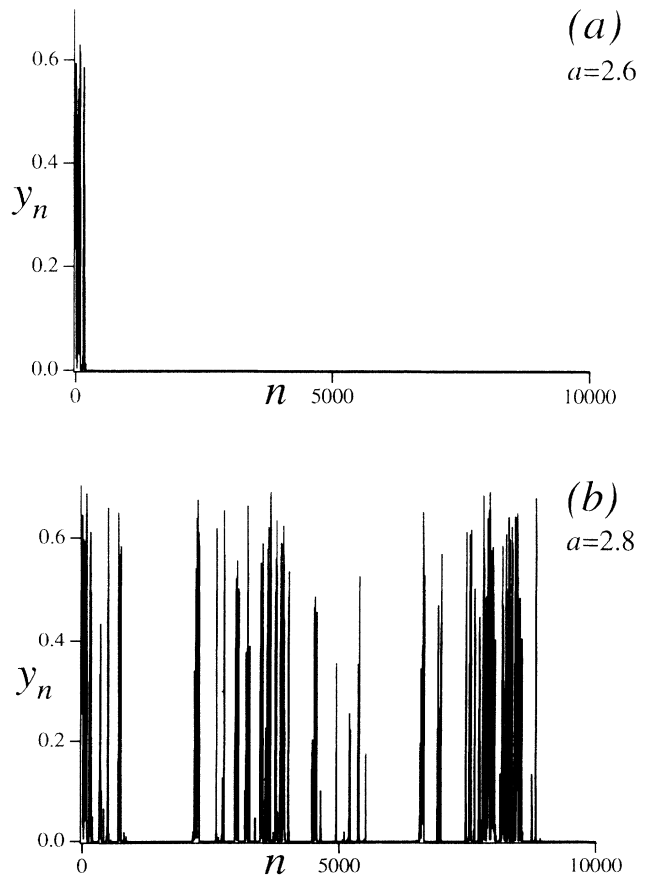


FIG. 4. Time series of driven logistic map with $2x_n \text{ mod } 1$ forcing: (a) below intermittency threshold at $a = 2.6$ and (b) above intermittency threshold at $a = 2.8$.

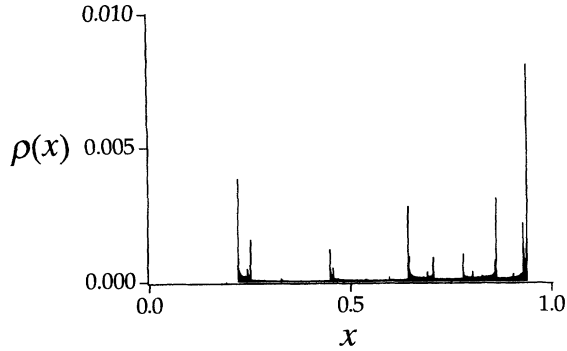


FIG. 5. Coarse-grained invariant density for logistic map at $\alpha=3.75$.

Like the map $x_{n+1}=2x_n \bmod 1$, the tent map also has uniform invariant measure in $(0,1)$ [20], and therefore yields a critical value of $a_c=e$ [21].

For more realistic chaotic driving choices, the invariant density of the driving variable is rarely known in closed form. An example is map (1) with $f(y_n)=y_n(1-y_n)$ and $z_n=ax_n$, where x_n also comes from a logistic map: $x_{n+1}=\alpha x_n(1-x_n)$. Similar maps (with two-way coupling) have been studied in [22,23]. The invariant density of x for $\alpha=3.75$ is shown in Fig. 5. The density was generated by forming the histogram of the iterates of a randomly chosen initial condition for 10^7 iterates. The width of each bin is 2×10^{-4} . The change of variable $z=ax$ in Eq. (6) leads to

$$\langle \ln z \rangle = \ln a + \int_0^1 \ln(x) \rho(x) dx, \quad (10)$$

where $\rho(x)$ is the invariant density of x . The integral in (10) can be approximated by employing the coarse-grained invariant density shown in Fig. 5. We find

$$\int_0^1 \ln(x) \rho(x) dx \approx -0.5146. \quad (11)$$

The critical value of a , obtained by solving $\langle \ln z \rangle = 0$, is found to be $a_c \approx 1.673$. Figures 6(a) and 6(b) show two time series for parameter values $a=1.66$ and 1.68 started from the same initial conditions. The onset prediction is again supported by the Figures. Similar results are expected to hold for other chaotic driving choices.

III. DISTRIBUTION OF LAMINAR PHASES: RANDOM DRIVING

The distinguishing characteristic of intermittent signals, such as those shown in Figs. 2, 4, and 6, is the time between successive ‘‘on’’ events, or large-amplitude bursts. The distribution of interevent times, or laminar phases, is easily measured, and serves as a potential classifier of the intermittent signal. This section is devoted to this distribution. We first analyze the random driving case. This analysis leads to an integro-difference equation whose solution is necessary to obtain the distribution of laminar phases. This equation is solved exactly for the case of uniformly distributed random driving. Asymptotic power-law behavior in the laminar phase distribution at onset is derived from this solution. Readers

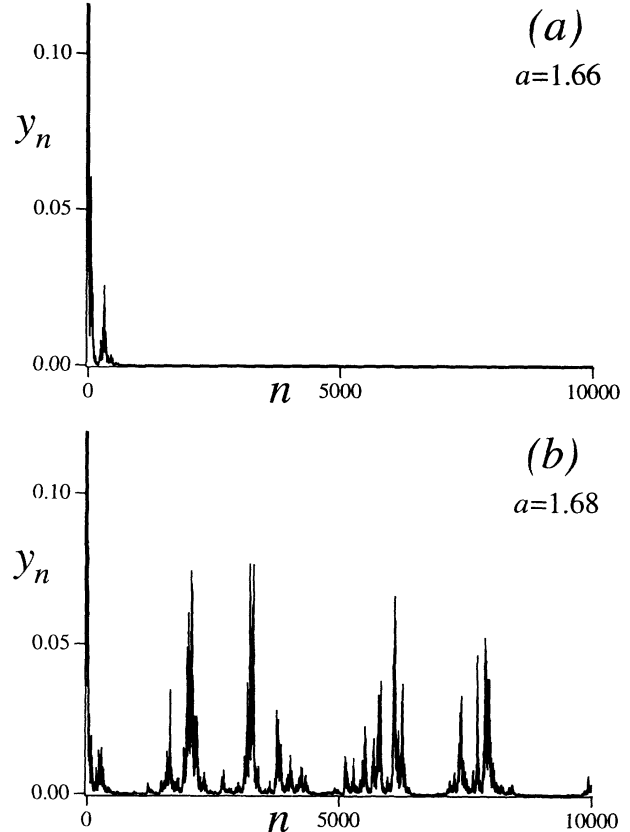


FIG. 6. Time series of driven logistic map with logistic map forcing with $\alpha=3.75$: (a) below intermittency threshold at $a=1.66$ and (b) above intermittency threshold at $a=1.68$.

interested in more general cases are urged to consult Sec. IV where, using random-walk methods, the universality of asymptotic power-law behavior at onset is proved for arbitrary random driving.

Let τ be a small threshold below which the signal y_n is considered to be ‘‘off.’’ A laminar phase of length n is defined by

$$\{y_1 \leq \tau, y_2 \leq \tau, \dots, y_n \leq \tau, y_{n+1} > \tau\}$$

(for a suitably shifted time origin). We are interested in the following probability: Given that we observe a laminar phase (i.e., at least length 1), what is the probability that it has exactly length n ? This is expressed by the conditional probability

$$\Lambda_n = \text{Prob} \left[\bigcap_{j=1}^n y_j \leq \tau \cap y_{n+1} > \tau \mid y_1 \leq \tau \right]. \quad (12)$$

A laminar phase is an event *local* to the fixed point at $y=0$. For this reason we assume that the laminar phases can be predicted from the linearized map (2). For thresholds τ that are small enough to be within the linear domain of the map [$\tau \ll \frac{1}{2} f''(0) \tau^2$], this assumption is justified. Ultimate justification comes from the numerical calculations that follow the analysis. There is no loss of generality in assuming $y_0 = \tau$. Under these assumptions, a laminar phase of length n corresponds to an event for

which the product P_k in (4) remains less than or equal to unity for exactly n iterations, and becomes greater than unity on the $n + 1$ st iteration. The probability (12) is therefore given by

$$\Lambda_n = \text{Prob} \left[\bigcap_{j=1}^n P_j \leq 1 \cap P_{n+1} > 1 \mid P_1 \leq 1 \right]. \tag{13}$$

Using the decomposition rule

$$\text{Prob}(A|B) = \text{Prob}(A \cap B) / \text{Prob}(B)$$

for events A and B , Λ_n can be written as

$$\Lambda_n = \frac{\text{Prob} \left[\bigcap_{j=1}^n P_j \leq 1 \cap P_{n+1} > 1 \right]}{\text{Prob}(P_1 \leq 1)}. \tag{14}$$

Since $P_1 = z_0$, the denominator of (14) is simply

$$\text{Prob}(P_1 \leq 1) = \int_{z_L}^1 \rho_z(z) dz. \tag{15}$$

It is convenient to define the event

$$E_n = \bigcap_{j=1}^n P_j \leq 1$$

and the corresponding probability

$$\lambda_n = \text{Prob}(E_n). \tag{16}$$

From the identity

$$\text{Prob}(E_n \cap P_{n+1} > 1) + \text{Prob}(E_n \cap P_{n+1} \leq 1) = \text{Prob}(E_n) \tag{17}$$

and the definition of λ_n , it follows that the numerator of (14) can be written as

$$\text{Prob}(E_n \cap P_{n+1} > 1) = \lambda_n - \lambda_{n+1}. \tag{18}$$

The problem is therefore reduced to calculating the probability λ_n .

We restrict the present study to cases where the driving variable z_n can be written as $z_n = ax_n$, where x_n is a random variable in $[0, 1]$ with density $\rho(x)$. In these cases the integrals required to calculate (16) simplify considerably.

The first step in computing λ_n is to perform the change of variables

$$\lambda_n = \int_{n \ln a}^{\infty} e^{-w_n} dw_n \int_{(n-1) \ln a}^{w_n} \rho(e^{-(w_n - w_{n-1})}) dw_{n-1} \int_{(n-2) \ln a}^{w_{n-1}} \rho(e^{-(w_{n-1} - w_{n-2})}) dw_{n-2} \cdots \times \int_{\ln a}^{w_2} \rho(e^{-(w_2 - w_1)}) \rho(e^{-w_1}) dw_1 \tag{25}$$

for $n \geq 2$. This can be written as

$$\lambda_n = \int_{n \ln a}^{\infty} e^{-w} \theta_{n-1}(w) dw, \tag{26}$$

where the function $\theta_n(w)$ satisfies the Volterra-type

$$\begin{aligned} w_1 &= -\ln x_0, \\ w_2 &= -(\ln x_0 + \ln x_1), \\ &\vdots \\ w_n &= -(\ln x_0 + \ln x_1 + \cdots + \ln x_{n-1}). \end{aligned} \tag{19}$$

This transforms the n -dimensional unit hypercube to the region described by $w_1 \geq 0$, $w_{k+1} \geq w_k$, for $k = 1, 2, \dots, n - 1$. The probability λ_n is then given by

$$\begin{aligned} \lambda_n &= \text{Prob} \left[\bigcap_{j=1}^n a^j \prod_{k=0}^{j-1} x_k \leq 1 \right] \\ &= \text{Prob} \left[\bigcap_{j=1}^n w_j \geq j \ln a \right]. \end{aligned} \tag{20}$$

To compute λ_n using (20), the joint density $F_w(w_1, w_2, \dots, w_n)$ is required. This is obtained from the joint density $F_x(x_1, x_2, \dots, x_n)$ through the transformation rule

$$F_w(w_1, w_2, \dots, w_n) = \frac{F_x(x_0, x_1, \dots, x_{n-1})}{|J|}, \tag{21}$$

where J is the Jacobian of the transformation (19); J is given by

$$J = \begin{vmatrix} \frac{\partial w_1}{\partial x_0} & \cdots & \frac{\partial w_1}{\partial x_{n-1}} \\ \vdots & & \vdots \\ \frac{\partial w_n}{\partial x_0} & \cdots & \frac{\partial w_n}{\partial x_{n-1}} \end{vmatrix} = \frac{(-1)^n}{x_0 x_1 \cdots x_{n-1}} = (-1)^n e^{w_n}, \tag{22}$$

where the last step follows from the definition of w_n in Eq. (19). The x 's are assumed to be independent, so the joint density F_x factors, yielding

$$\begin{aligned} F_w(w_1, w_2, \dots, w_n) &= \frac{\rho(x_0) \rho(x_1) \cdots \rho(x_{n-1})}{|J|} \\ &= e^{-w_n} \rho(e^{-w_1}) \rho(e^{-(w_2 - w_1)}) \\ &\quad \times \cdots \rho(e^{-(w_n - w_{n-1})}). \end{aligned} \tag{23}$$

Figure 7 shows the integration domain for the calculation of λ_2 ; the integral is given by

$$\lambda_2 = \int_{2 \ln a}^{\infty} e^{-w_2} dw_2 \int_{\ln a}^{w_2} \rho(e^{-(w_2 - w_1)}) \rho(e^{-w_1}) dw_1. \tag{24}$$

In the general case the integral appears as

integro-difference equation [24]

$$\theta_n(w) = \int_{n \ln a}^w \rho(e^{-(w - \xi)}) \theta_{n-1}(\xi) d\xi, \tag{27a}$$

with

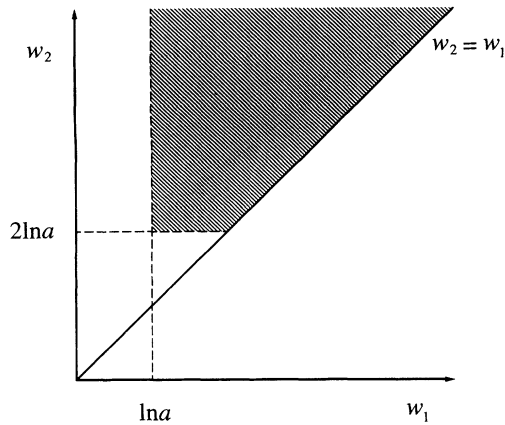


FIG. 7. Integration domain (shaded) in w_1 - w_2 plane for the calculation of λ_2 .

$$\theta_1(w) = \int_{\ln a}^w \rho(e^{-(w-\xi)}) \rho(e^{-\xi}) d\xi. \quad (27b)$$

To our knowledge, a closed-form solution of Eq. (27) for arbitrary $\rho(x)$ is not available. A solution can be found, however, for certain simple forms of $\rho(x)$. In the following we carry out the solution for the case studied in Sec. I, $\rho(x) \equiv 1$. In this case Eq. (27a) can be converted to a differential-difference equation by differentiating both sides with respect to w . One gets

$$\dot{\theta}_n(w) = \theta_{n-1}(w), \quad (28a)$$

with

$$\theta_n(n \ln a) = 0. \quad (28b)$$

The solution of this equation is facilitated by taking Laplace transforms. Let $H_n(s)$ denote the Laplace transform of $\theta_n(w)$. The Laplace transform of Eq. (28a) then yields the difference equation

$$sH_n(s) - \theta_n(0) = H_{n-1}(s), \quad (29)$$

whose solution is

$$H_n(s) = \frac{H_1(s)}{s^{n-1}} + \sum_{i=2}^n \frac{\theta_i(0)}{s^{n+1-i}}. \quad (30)$$

$H_1(s)$ is easily computed from Eq. (27b) and leads to

$$H_1(s) = \frac{1}{s^{n+1}} - \frac{\ln a}{s^n} + \sum_{i=2}^n \frac{\theta_i(0)}{s^{n+1-i}}. \quad (31)$$

The inverse Laplace transform of (31) gives

$$\theta_n(w) = \frac{w^n}{n!} - \frac{(\ln a)w^{n-1}}{(n-1)!} + \sum_{i=2}^n \frac{\theta_i(0)w^{n-i}}{(n-i)!}. \quad (32)$$

Enforcing the conditions $\theta_n(n \ln a) = 0$, it is easily verified that $\theta_i(0) = 0$ for $i \geq 2$, so the sum in (32) is zero. Substituting $\theta_{n-1}(w)$ into (26) and integrating, one obtains, after some simplification,

$$\lambda_n(a) = \frac{1}{a^n} \left[\frac{(\ln a)^{n-1} n^n}{n!} + (1 - \ln a) \sum_{j=0}^{n-2} \frac{(n \ln a)^j}{j!} \right]. \quad (33)$$

For $\rho(x) = 1$, Eqs. (13), (14), and (17) give

$$\Lambda_n = a(\lambda_n - \lambda_{n+1}). \quad (34)$$

The probability of a laminar phase of length n is found by combining (33) with (34). The normalization of the distribution of laminar phases is easily verified:

$$\sum_{n=1}^{\infty} \Lambda_n = a \sum_{n=1}^{\infty} (\lambda_n - \lambda_{n+1}) = a \lambda_1 = 1. \quad (35)$$

A similar analysis can be carried out for the class of density functions $\rho(x) = (k+1)x^k$, $k \geq 0$. In this case the critical parameter is $a_c = e^{1/(k+1)}$ and the distribution of laminar phases is obtained by letting $a \rightarrow a^{k+1}$ in Eqs. (33) and (34).

We are primarily interested in cases at and just beyond the onset of intermittency, i.e., $a \geq a_c = e$. We first examine the onset probability $\Lambda_n(e)$, which is given by

$$\Lambda_n(e) = \frac{e n^n}{e^n n!} \left[1 - \frac{(1+1/n)^n}{e} \right]. \quad (36)$$

Applying Stirling's formula for $n!$, $n! \sim \sqrt{2\pi n} e^{-n} n^n$, and the asymptotic relation

$$(1+1/n)^n \sim e(1-1/2n),$$

one obtains the asymptotic probability

$$\Lambda_n(e) \sim \frac{e}{2\sqrt{2\pi}} n^{-3/2}. \quad (37)$$

At onset the distribution of laminar phases is a power law with exponent $-\frac{3}{2}$. It follows that there is no characteristic time scale and there are laminar phases of arbitrarily long length. In particular, the average laminar phase is infinite.

Beyond onset, the leading-order asymptotic behavior of Λ_n can be found by keeping only the largest term in the sum (33) for λ_n , which for $a \geq e$ is the $j = n-2$ term. This yields

$$\lambda_n(a) = \frac{1}{a^n} \frac{(\ln a)^{n-1} n^n}{n!} \left[\frac{1}{\ln a} + O(n^{-1}) \right]. \quad (38)$$

Λ_n then becomes

$$\begin{aligned} \Lambda_n(a) &\approx \frac{a}{(\ln a)^2} \frac{(\ln a)^n n^n}{a^n n!} \left[1 - \frac{\ln a}{a} \left[1 + \frac{1}{n} \right]^n \right] \\ &\sim \frac{a}{(\ln a)^2} \frac{e^{n(1+\ln(\ln a) - \ln a)}}{\sqrt{2\pi n}} \\ &\quad \times \left[1 - \frac{e \ln a}{a} \left[1 - \frac{1}{2n} \right] \right], \end{aligned} \quad (39)$$

where Stirling's approximation has been applied in the second equation. Since we are interested in cases near onset, we put $a = e + \delta$ and expand Eq. (39) to leading order in δ . The result is

$$\Lambda_n \sim \frac{e}{2\sqrt{2\pi}} \exp \left[-\frac{n\delta^2}{2e^2} \right] n^{-3/2}. \quad (40)$$

Beyond onset the exponential decay with n insures a finite

mean laminar phase (see Sec. VI below). The e -folding time of the exponential decay defines a characteristic time: $n_c = 2e^2/\delta^2$. For $n < n_c$, the $-\frac{3}{2}$ power law dominates, while for $n > n_c$, the exponential decay dominates.

Figure 8(a) shows a plot of Λ_n determined from a numerical simulation of the randomly driven logistic map with $a = 2.75$ [25]. A total of 500 000 laminar phases were used to construct the distribution. The threshold for a laminar phase was fixed at $\tau = 0.001$ (essentially identical results were found for $\tau = 0.01$). Superimposed on the distribution is the theoretical distribution (34) (solid line) and the asymptotic distribution (40) (dashed line). Since the characteristic time for $a = 2.75$ is $n_c \approx 2213$, the exponential decay is not observed. This figure confirms the theoretical predictions for the uniform random driving case. We have also carried out similar numerical experiments with a variety of random driving densities $\rho(x)$ (e.g., $\sin(\pi x)$, $\cosh[\alpha(x - \frac{1}{2})]$, $\exp(-\alpha x)$, with suitable normalization factors). Just beyond onset, for all cases studied, the asymptotic distribution of laminar phases fits well to a power law with exponent $-\frac{3}{2}$, as in the uniform driving case. From these results it is apparent that the linearized map (2) is sufficient to explain the laminar phase distribution.

IV. UNIVERSALITY IN THE LAMINAR PHASE DISTRIBUTION

In this section we show that the asymptotic power-law behavior in the distribution of laminar phases is a *universal* feature of on-off intermittency in map (1) for a large class of random driving cases. For this analysis we rely on some results from the theory of random walks. Equation (2) describes an additive random walk in the log domain:

$$s_{n+1} = q_n + s_n, \quad (41)$$

where $s_n = \ln(y_n)$, $q_n = \ln(z_n)$, and the steps q_n have density $\rho_q(q) = e^q \rho_z(e^q)$. In this setting the onset condition $\langle \ln z \rangle = \langle q \rangle = 0$ has a straightforward interpretation—the random walk is *unbiased*. Since (41) is translationally invariant, without loss of generality, we can take $s_0 = 0$. The distribution of laminar phases (12) is then equivalent to the following probability:

$$\Lambda_n = \text{Prob} \left[\bigcap_{j=1}^n s_j \leq 0 \cap s_{n+1} > 0 \mid s_1 \leq 0 \right]. \quad (42)$$

Let

$$g_n = \text{Prob} \left[\bigcap_{j=1}^n s_j \leq 0 \right].$$

Following a similar argument to that used in obtaining Eq. (18), Λ_n is given by

$$\Lambda_n = \frac{g_n - g_{n+1}}{\text{Prob}(s_1 \leq 0)}. \quad (43)$$

To compute g_n , we appeal to a theorem from the theory of random walks. Define a generating function for the probability g_n :

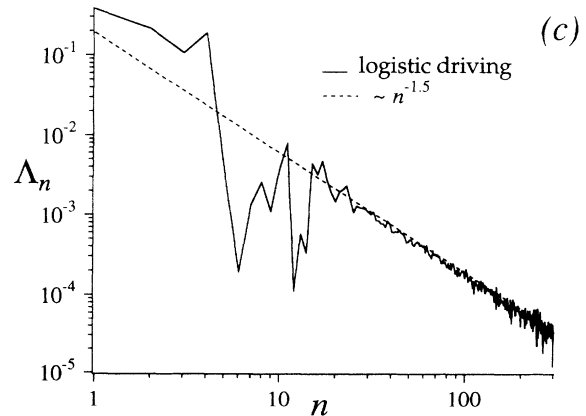
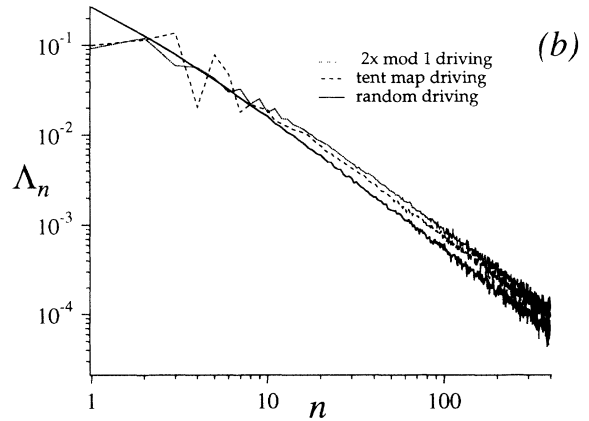
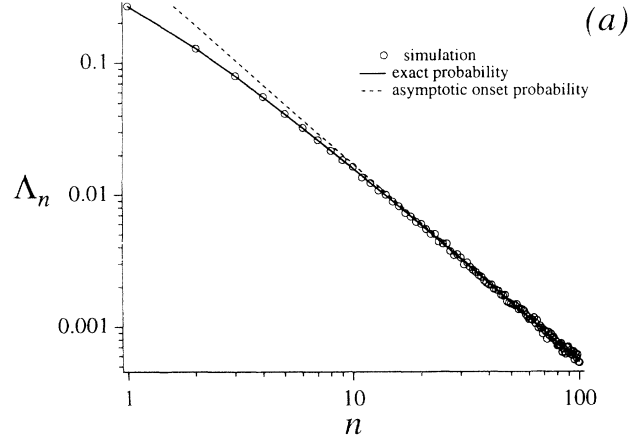


FIG. 8. Distribution of laminar phases: (a) Uniform random driving at $a = 2.75$. The circles are from simulation, the solid line is the exact distribution from Eq. (34), and the dashed line is the asymptotic power law of Eq. (40). (b) Comparison of $2x \bmod 1$ driving (dotted), tent-map driving (dashed), and uniform random driving (solid), all for $a = 2.75$. (c) Logistic map driving at $\alpha = 3.75$ and $\alpha = 1.675$ (solid). Shown for comparison is a $-\frac{3}{2}$ power law (dashed).

$$G(t) = \sum_{n=0}^{\infty} g_n t^n. \quad (44)$$

Then the following theorem holds:

$$\ln[G(t)] = \sum_{n=1}^{\infty} \frac{t^n}{n} \text{Prob}(s_n \leq 0). \quad (45)$$

This theorem relates the probability of the particle being in the left half-line at the n th step to the desired probability g_n , through the generating function $G(t)$. A proof of this theorem can be found in Feller [26].

First consider the case where $\rho_q(q)$ is symmetric; $\rho_q(-q) = \rho_q(q)$. In this case the probability of being to the left of the origin at the n th step must equal the probability of being to the right of the origin at the n th step, so $\text{Prob}(s_n \leq 0) = \frac{1}{2}$. The sum on the right-hand side of (45) can then be evaluated exactly (differentiate the sum, sum the resulting the geometric series, and integrate):

$$\frac{1}{2} \sum_{n=1}^{\infty} \frac{t^n}{n} = \ln \left[\frac{1}{\sqrt{1-t}} \right]. \quad (46)$$

The generating function is therefore given by

$$G(t) = \frac{1}{\sqrt{1-t}}. \quad (47)$$

The coefficients g_n are determined through the relations

$$g_n = \frac{1}{n!} \left. \frac{\partial^n G(t)}{\partial t^n} \right|_{t=0}. \quad (48)$$

Carrying out the derivatives, one finds

$$g_n = \frac{(2n)!}{2^{2n}(n!)^2}. \quad (49)$$

A straightforward calculation shows that the numerator of (43) is given by

$$g_n - g_{n+1} = \frac{g_n}{2(n+1)} \sim \frac{1}{2\sqrt{\pi}} n^{-3/2}, \quad (50)$$

where the last relation follows from Stirling's approximation. We conclude that, at onset, Λ_n decays as a power law with exponent $-\frac{3}{2}$.

This result can be extended to include all densities ρ_q with zero mean and finite variance. These cases are expected to be met most frequently in practice (all of the cases discussed in this paper fall within this class). Density functions with zero mean and finite variance satisfy the relation

$$\sum_{n=1}^{\infty} \frac{1}{n} [\text{Prob}(s_n \leq 0) - \frac{1}{2}] = c, \quad (51)$$

for some bounded constant c (for symmetric densities, $c=0$). For a proof of this relation, see [26].

Subtracting

$$\ln \left[\frac{1}{\sqrt{1-t}} \right] = \frac{1}{2} \sum_{n=1}^{\infty} \frac{t^n}{n}$$

from both sides of Eq. (45) one obtains

$$\ln[G(t)\sqrt{1-t}] = \sum_{n=1}^{\infty} \frac{t^n}{n} [\text{Prob}(s_n \leq 0) - \frac{1}{2}]. \quad (52)$$

In the limit $t \rightarrow 1$, the right-hand side of this expression is c . Therefore, as $t \rightarrow 1$,

$$G(t) \sim \frac{e^c}{\sqrt{1-t}}. \quad (53)$$

To obtain the asymptotic behavior of the coefficient g_n , we appeal to a theorem from asymptotic analysis. Let $G(t) = \sum_{n=0}^{\infty} g_n t^n$ converge for $0 \leq t < 1$ and let the sequence $\{g_n\}$ be monotonic with $g_n \geq 0$ (these conditions hold for g_n). Then the relations

$$G(t) \sim \frac{\alpha}{(1-t)^\rho} \quad (54a)$$

and

$$g_n \sim \frac{\alpha}{\Gamma(\rho)} n^{\rho-1}, \quad (54b)$$

where $\rho \geq 0$, $0 < \alpha < \infty$, and Γ is the gamma function, imply one another (see [26]). Applying this theorem to the generating function $G(t)$ in (53) gives

$$g_n \sim \frac{e^{-c}}{\sqrt{\pi}} n^{-1/2}. \quad (55)$$

Finally, the numerator of (43) becomes

$$g_n - g_{n+1} \sim g_n \left[1 - \left(1 + \frac{1}{n} \right)^{-1/2} \right] \sim \frac{e^{-c}}{2\sqrt{\pi}} n^{-3/2}, \quad (56)$$

and it follows that $\Lambda_n \sim n^{-3/2}$, as claimed.

Beyond onset, we expect the distribution of laminar phases to decrease exponentially with n as $n \rightarrow \infty$, as was found for the uniform driving case in Sec. III.

V. DISTRIBUTION OF LAMINAR PHASES: CHAOTIC DRIVING

In this section we consider the distribution of laminar phases for cases with chaotic driving. The laminar phase analysis presented in Sec. III cannot be applied to these cases because the assumption of independence does not hold for chaotic driving; correlations are always present in chaotic time series. As a result, the joint density F_x in Eq. (23) cannot be factored. Independence is also assumed in the proof of (45) so the general random-walk analysis of Sec. IV cannot be applied.

Figure 8(b) shows Λ_n for three cases: uniform random driving, $2x \bmod 1$ driving, and tent-map driving. Parameters were again $a=2.75$ and $\tau=0.001$. We collected 500 000 laminar phases for each distribution. The striking feature of Fig. 8(b) is the asymptotic behavior of the two chaotic driving cases, each of which approach a $-\frac{3}{2}$ power law (with slightly different multiplicative constants). This is surprising in light of the fact that the random driving analysis does not hold for chaotic driving. The close agreement between the $2x \bmod 1$ and tent-map results for $n=1$ and 2 is due to their common definition for $0 \leq x \leq \frac{1}{2}$.

Figure 8(c) shows the distribution of laminar phases for map (1) with logistic map driving at $\alpha=1.675$. Again, the distribution approaches a $-\frac{3}{2}$ power law. Evidently, the asymptotic $-\frac{3}{2}$ power law can be explained within the context of a more general theory, which does not make explicit use of the independence of the driving variable. We return to this idea in Sec. VII.

VI. AVERAGE LAMINAR PHASE BEYOND ONSET

A commonly used signature in intermittency studies is the average laminar phase [2,4,8]. Of particular interest is the behavior of the mean laminar phase as a function of a map parameter. Here we study the mean laminar phase as a function of the coupling parameter a .

For uniform random driving, the mean laminar phase can be computed directly from the distribution (34):

$$\langle n \rangle = \sum_{n=1}^{\infty} n \Lambda_n = a \sum_{n=1}^{\infty} n (\lambda_n - \lambda_{n+1}) = a \sum_{n=1}^{\infty} \lambda_n. \quad (57)$$

To our knowledge, the sum $\sum_{n=1}^{\infty} \lambda_n$ cannot be expressed in closed form. Near onset, an approximate expression for the mean laminar phase can be obtained as follows. We are interested in the leading-order behavior of the mean laminar phase in terms of the deviation $\delta = a - e$. Since δ controls the tail of the laminar phase distribution [see the asymptotic formula (40)], it is reasonable to expect that the leading-order behavior can be obtained by substituting Eq. (40) into the first sum in (57) and converting the sum to an integral. Carrying this out, one gets

$$\begin{aligned} \langle n \rangle &= \sum_{n=1}^{\infty} n \Lambda_n \approx \frac{e}{2\sqrt{2\pi}} \int_1^{\infty} \exp\left[\frac{-n\delta^2}{2e^2}\right] n^{-1/2} dn \\ &= \frac{e^2}{2\delta} \left[1 - \operatorname{erf}\left[\frac{\delta}{e\sqrt{2}}\right] \right] \\ &= \frac{e^2}{2\delta} \left\{ 1 - \frac{2}{\sqrt{\pi}} \left[\frac{\delta}{e\sqrt{2}} + O\left(\frac{\delta}{e\sqrt{2}}\right)^3 \right] \right\} \\ &\approx \frac{e^2}{2\delta} - \frac{e}{\sqrt{2\pi}}. \end{aligned} \quad (58)$$

Apart from an additive constant, the predicted mean laminar phase is a power law near $a=e$, with a critical exponent of -1 .

Figure 9(a) shows the numerically determined mean laminar phase as a function of δ for the logistic map with random driving, $2x \bmod 1$ driving, and tent-map driving. We kept 100 000 laminar phases for each value of δ for all runs. The quantity that is plotted is $\langle n \rangle - c_0$, where c_0 is determined from a least-squares fit to the model $\langle n \rangle = c_0 + c_1/\delta$. The fit for the random case (solid line) gives parameters $c_0 = 1.27$ and $c_1 = 3.62$; the coefficient c_1 is in good agreement with the theoretical prediction of (58), $(c_1)_{\text{theor}} \approx 3.69$. Coefficients for the other cases are listed in the inset to Fig. 9(a). All cases clearly show power-law scaling of the mean laminar phase near $a=e$, with a critical exponent of -1 .

Figure 9(b) shows the mean laminar phase as function

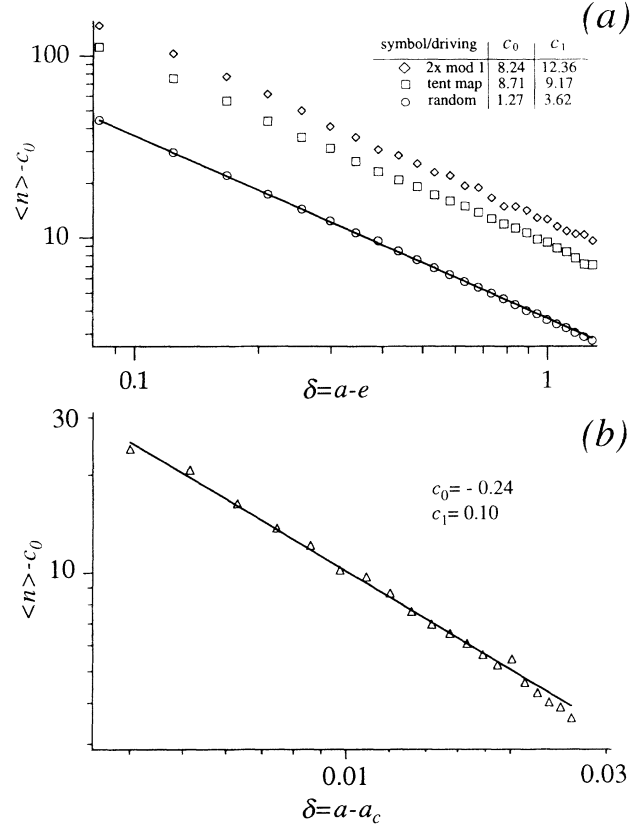


FIG. 9. Mean laminar phase as a function of deviation from critical onset parameter $\delta = a - a_c$: (a) Comparison of $2x \bmod 1$ (triangles), tent map (squares), and uniform random driving (circles). The solid line is best fit to random driving case and (b) logistic map driving at $\alpha = 3.75$. The solid line is best fit to model $\langle n \rangle = c_0 + c_1/\delta$.

of $a - a_c$ ($a_c = 1.673$) for logistic map driving. The solid line is a least-squares fit to the model $\langle n \rangle = c_0 + c_1/\delta$. Again, this model is a good representation of the mean laminar phase near onset. These results point strongly toward a universal power-law behavior in the mean laminar phase beyond onset, for both random and chaotic driving cases.

VII. SUMMARY AND DISCUSSION

In this study we have characterized the statistical properties of on-off intermittent signals in a simple class of parametrically driven one-dimensional maps. At the onset of intermittent behavior, the distribution of laminar phases for a large class of random driving cases exhibits a universal asymptotic $-\frac{3}{2}$ power law. For uniformly distributed random driving, an analytic expression for this distribution has been obtained. Asymptotic power-law behavior has also been found numerically in all of the chaotic driving cases we have considered. We expect this to be a typical feature of chaotic driving cases.

Just beyond onset, the mean laminar phase for both random and chaotic driving cases has been found to display power-law scaling as a function of the coupling strength, with a critical exponent of -1 . For uniformly

distributed random driving, this result has been supported analytically.

An immediate question prompted by these results is the following: Is there a setting in which to understand both the random and the chaotic driving cases? We suggest that one approach to answering this question is through the study of "chaotic walks," i.e., additive walks where the increments are chosen from some chaotic process. We know of no systematic studies of chaotic walks, though they are clearly an important counterpart to the comparatively well studied random walks. It would be useful to know, for example, under what conditions a chaotic walk can be approximated by a random walk, and vice versa. Heuristically, one expects chaotic processes with sufficiently large Lyapunov exponents to qualify as random processes, but there is a need to put this and similar ideas on a firm mathematical foundation. Also of use would be limit theorems, similar in spirit to the central limit theorem, and to the theorem of Eq. (45), for sums of chaotic variables. Such theorems would allow one to address directly the asymptotic behavior of the distribution of laminar phases for chaotic driving. Some results along these lines can be found in Beck [27].

It is important to compare on-off intermittency to other intermittency theories. We briefly discuss these comparisons here. A common ingredient in all theories of intermittency is *bifurcation*. Type-I, -II, and -III intermittency each result from local bifurcations; each type corresponds to a unique way for the eigenvalues of a fixed point to pass through the unit circle [2]. Crisis-induced intermittency arises from a global bifurcation—a crisis [7,8]. The intermittent behavior in all of these theories occurs for *fixed* parameter values, just beyond the bifurcation point. In contrast, on-off intermittency is triggered by modulating a parameter through a local bifurcation. On-off intermittency is then effectively *dynamic* in parameter space, while type-I, -II, -III, and crisis-induced intermittencies are all *static*.

The distribution of laminar phases differs between different types of intermittency. A helpful summary of results for type-I, -II, and -III intermittency can be found in Schuster [20]. Type-III intermittency is especially of interest. As in on-off intermittency, the distribution of laminar phases just beyond onset is a $-\frac{3}{2}$ power law for short laminar phases, and eventually turns over to an exponential falloff with n as $n \rightarrow \infty$. Also like on-off intermittency, the mean laminar phase beyond onset decays as δ^{-1} , where δ is the distance from the onset parameter. Thus, in distinguishing between type-III intermittency and on-off intermittency in experiments, it is important to consider not just the measured properties, but the mechanism for the intermittent behavior as well. Type-III intermittency requires a flip saddle. Because of this, the intermittent signals exhibit bursts about either side of the fixed point, giving a characteristic appearance [20] which can aid in the identification of type-III intermittency. Type-I and -II intermittency have power-law laminar phase distributions initially, but with power laws $-\frac{1}{2}$ and -2 , respectively. The mean laminar phase scales as

$\delta^{-1/2}$ and δ^{-1} for type-I and -II, respectively. These types of intermittent behavior are therefore distinguishable from on-off intermittency. Finally, crisis-induced intermittency should be easily distinguished from on-off intermittency. The "laminar phases" in crisis-induced intermittency are segments of chaotic orbits representing jumps between former separate attractors. In contrast, the laminar phases in on-off intermittency are nonchaotic (fixed points or periodic orbits).

Recently, Yu, Ott, and Chen [12,13] have studied a class of two-dimensional maps with randomly varying parameters. These maps, which model the dynamics of passive scalars on the surface of a fluid, exhibit so-called snapshot attractors. Snapshot attractors can undergo a form of intermittent behavior that is similar to on-off intermittency. There are some essential differences between the behavior of snapshot attractors and the attractors studied in this paper, however. The intermittent "signal" in the maps in [12] and [13] is the *size* of the snapshot attractor as the map is iterated; the size is computed as an rms average over the attractor at each map iterate for a large ensemble of initial conditions. For our maps we can also define a size distribution by forming the histogram of y values. Because this distribution is independent of the time ordering of the y values, the size distribution is, in general, *independent* of the distribution of laminar phases. The size distribution of snapshot attractors computed in Refs. [12] and [13] is quite different from the laminar phase distribution found in this paper. We add that from an experimental point of view, it may be preferable to measure the laminar phase distribution over the size distribution because of the expected insensitivity of the former to noise.

The results of this paper are based entirely on the dynamics of a class of one-dimensional maps without noise. These maps are obviously idealized, and experimental systems would no doubt require more realistic models. External noise has been shown to have significant effects in other theories of intermittency [3,4,6,28,29]. Preliminary investigations show this to be true for on-off intermittency as well; we will report on external noise effects in a future work. Finally, it is important to extend the theory to higher dimensional systems and to systems in continuous time, both of which we hope to report on in the near future.

Note added in proof. After submitting this paper we learned of related work by the following authors: H. Fujisaka and T. Yamada, Prog. Theor. Phys. **74**, 918 (1985); **77**, 1045 (1987); A. S. Pikovsky, Phys. Lett. A **165**, 33 (1992). We thank E. Ott and J. Sommerer for bringing these references to our attention.

ACKNOWLEDGMENTS

Many thanks go to John Barnett for several informative discussions. J.H. is supported by NRC and gratefully acknowledges support from ONR. N.P. is supported by ONT/ASEE. We thank the NSWC Seed and Ventures Program for partial support.

- [1] N. Platt, E. A. Spiegel, and C. Tresser, *Phys. Rev. Lett.* **70**, 279 (1993).
- [2] Y. Pomeau and P. Manneville, *Commun. Math. Phys.* **74**, 189 (1980).
- [3] J. E. Hirsch, B. A. Huberman, and D. J. Scalapino, *Phys. Lett. A* **87**, 391 (1982).
- [4] J. E. Hirsch, B. A. Huberman, and D. J. Scalapino, *Phys. Rev. A* **25**, 519 (1982).
- [5] E. N. Lorenz, *J. Atmos. Sci.* **20**, 130 (1963).
- [6] B. Hu and J. Rudnick, *Phys. Rev. Lett.* **48**, 1645 (1982).
- [7] C. Grebogi, E. Ott, and J. A. Yorke, *Phys. Rev. Lett.* **48**, 1507 (1982).
- [8] C. Grebogi, E. Ott, F. J. Romeiras, and J. A. Yorke, *Phys. Rev. A* **36**, 5365 (1987).
- [9] Here and throughout this paper we treat $\rho_z(z)$ as a continuous function, although there are clearly cases where it is not continuous (for instance, chaotic processes typically have discontinuous density functions). Our results appear to hold for these cases, as well. We have chosen to treat $\rho_z(z)$ as a continuous function to avoid the more rigorous, but perhaps less familiar, notation employing probability measures.
- [10] S. J. Linz and M. Lücke, *Phys. Rev. A* **33**, 2694 (1986).
- [11] The random number generator used for all our numerical work is taken from S. K. Park and K. W. Miller, *Commun. ACM* **31**, 1192 (1988).
- [12] L. Yu, E. Ott, and Q. Chen, *Phys. Rev. Lett.* **65**, 2935 (1990).
- [13] L. Yu, E. Ott, and Q. Chen, *Physica D* **53**, 102 (1991).
- [14] If the density function is discontinuous, the integral (6) must be replaced by a Lebesgue integral over the probability measure $d\mu_z(z)$.
- [15] L. M. Pecora and T. L. Carroll, *Phys. Rev. Lett.* **64**, 821 (1990).
- [16] L. M. Pecora and T. L. Carroll, *Phys. Rev. A* **44**, 2374 (1991).
- [17] M. de Sousa Vieira, A. J. Lichtenberg, and M. A. Lieberman, *Int. J. Bifurc. Chaos* **1**, 691 (1991).
- [18] L. O. Chua, L. Kocarev, K. Eckert, and M. Itoh, *Int. J. Bifurc. Chaos* **2**, 705 (1992).
- [19] The map $x_{n+1} = 2x_n \bmod 1$ must be implemented with care. Direct floating-point implementation results in improper convergence to the unstable fixed point at $x = 0$ (for example, in a double-precision implementation with 64 bits of precision, x will converge to zero in about 64 iterations). To avoid this, we employ a well-known binary-shift technique on a finite binary array. At each iteration of the map, a left shift is performed on the array and the least significant element of the array is set to 1 or 0 randomly with equal probability.
- [20] H. G. Schuster, *Deterministic Chaos*, 2nd ed. (VCH, New York, 1989).
- [21] More rigorously, this onset condition must be supplemented with a condition on the correlation properties of the driving sequence $\{x_n\}$. Examples can be constructed where no intermittent behavior will be observed. One is the case for which a large value of x_n on one iterate (expansion) is countered by an approximate reciprocal contraction on the next iterate. Another example is the sequence generated from the map $x_{n+1} = x_n + \epsilon \bmod 1$, where ϵ is a small irrational number. The correlation condition is not needed for δ -function-correlated random driving (or tent-map driving, which is also δ correlated). For $2x \bmod 1$, the exponential decay of correlations is evidently sufficient to guarantee intermittency. A mathematically precise correlation condition that guarantees intermittent behavior for arbitrary driving signals is still outstanding.
- [22] J. M. Yuan, M. Tung, D. H. Feng, and L. M. Narducci, *Phys. Rev. A* **28**, 1662 (1983).
- [23] R. López-Ruiz and C. Pérez-García, *Chaos Solitons Fractals* **1**, 511 (1991).
- [24] T. L. Saaty, *Modern Nonlinear Equations* (Dover, New York, 1981).
- [25] In practice we add a small amount of noise to the map (of magnitude $\sim 10^{-300}$) at each iteration. This allows us to carry out simulations just above the critical value $a = a_c$. Such a small amount of noise does not affect the distribution of laminar phases in a fundamental way, although in a future paper we will show that higher noise levels do change the character of the distribution.
- [26] W. Feller, *An Introduction to Probability Theory and its Applications*, 2nd ed. (Wiley, New York, 1971), Vol. II.
- [27] C. Beck, *Physica A* **169**, 324 (1990).
- [28] J. P. Eckmann, L. Thomas, and P. Wittwer, *J. Phys. A* **14**, 3153 (1981).
- [29] J. C. Sommerer, E. Ott, and C. Grebogi, *Phys. Rev. A* **43**, 1754 (1991).